7. W. E. Armstrong and B. L. Tolliver, *This Journal*, **121**, 307 (1974).
8. E. Tanikawa, O. Takayama, and K. Maeda, in "Chemical Vapor Deposition," G. F. Wakefield and J. M. Blocher, Jr., Editors, p. 261, The Electrochemical Society Softbound Proceedings Series, Princeton, NJ (1973).
9. A. C. Adams and C. D. Capio, *This Journal*, **126**, 1042 (1979).
10. R. C. Archer, *J. Opt. Soc. Am.*, **52**, 970 (1962).
11. A. C. Adams, D. P. Schinke, and C. D. Capio, *This Journal*, **126**, 1539 (1979).
12. A. C. Adams and S. P. Murarka, *ibid.*, **126**, 334 (1979).
13. J. Monkoski and J. Stach, *Solid State Technol.*, **19**(11), 38 (1976).
14. B. J. Baliga and S. K. Ghandhi, *J. Appl. Phys.*, **44**, 990 (1973).
15. E. A. Taft, *This Journal*, **126**, 1728 (1979).
16. M. Shibata and K. Sugawara, *ibid.*, **122**, 155 (1975).
17. J. Middelhoeck and A. J. Klinkhamer, in "Chemical Vapor Deposition," J. M. Blocher, Jr., H. R. Hinterman, and L. H. Hall, Editors, p. 19, The Electrochemical Society Softbound Proceedings Series, Princeton, NJ (1975).
18. G. Wahl, in "Chemical Vapor Deposition," J. M. Blocher, Jr., H. R. Hinterman, and L. H. Hall, Editors, p. 391, The Electrochemical Society Softbound Proceedings Series, Princeton, NJ (1975).
19. M. Shibata, T. Yoshimi, and K. Sugawara, *This Journal*, **122**, 157 (1975).
20. A. C. Adams, C. D. Capio, S. H. Haszko, G. I. Parisi, E. I. Povilonis, and McD. Robinson, *ibid.*, **126**, 313 (1979).

A Model for Boron Deposition in Silicon Using a BBr_3 Source

S. F. Guo* and W. S. Chen

Institute of Electronics, National Chiao Tung University, Hsinchu, Taiwan, China

ABSTRACT

The sheet resistance and junction depth as a function of time at various temperatures have been obtained for the deposition of boron in silicon by using a BBr_3 liquid source. A simulation program incorporating a more realistic moving boundary condition is developed to analyze the deposition process under oxidizing atmosphere. By fitting numerical solutions to experimental data, the moving interface velocity and diffusion coefficient are determined. The profile of deposited layers as a function of doping gas composition can be modeled by the change of silicon self-interstitial concentration. The solid solubility of boron in silicon as a function of temperature has been determined. Different surface concentrations corresponding to different thicknesses of the boron-rich layer can be explained by the translation of the BRL-Si interface.

Boron tribromide (BBr_3) is the p-type dopant source most commonly used in silicon planar technology (1). Since the deposition of boron in silicon using BBr_3 is generally carried out in an oxidizing atmosphere, the physical process is more complicated than that using BN under inert ambient. A purely vacancy model gives a good prediction of the sheet resistance as a function of time for various temperatures when a boron nitride solid source is used (2). However, as shown in Fig. 1, the quantity of boron atoms deposited into silicon using BBr_3 is much larger than that using BN and is not increased linearly with the square root of time as predicted from a simple diffusion model (2).

It is well-known (3) that the diffusivity of boron in silicon depends not only on doping concentration but also on the oxidation rate of silicon at the surface. The concentration-dependent diffusion is generally modeled by a vacancy mechanism, while the oxidation-enhanced diffusion is related to the interstitialcy mechanism. In general, the vacancy contribution is determined from the multiple charge state vacancy statistics (2, 4) and the interstitialcy contribution is given as a function of oxidation rate (5, 6).

Naturally, the oxidation of silicon will consume silicon as well as some impurity atoms already deposited in it. The purpose of this paper is to show that the sheet resistance and junction depth as a function of time for various temperatures can be simulated by taking a moving boundary condition into account.

As shown by Negrini *et al.* (1), the deposition of boron in silicon using BBr_3 depends strongly on doping gas composition for a given temperature and time. However, for a suitably chosen doping gas composition, some reproducible results of sheet resistance and junction depth can be obtained. On the other hand, the increase of deposition quantity with oxygen flow rate can be modeled by the oxidation rate dependence of silicon self-interstitials (6), while the anomalous decrease of deposition quantity with BBr_3 flow rate can be explained by the reduction of the population of interstitial excess silicon in the $Si-SiO_2$ interface. The reaction of oxygen with silicon will generate some interstitial silicons (3) whose concentration will be reduced by interacting with boric oxide and bromine produced by the preliminary reaction of BBr_3 and O_2.

Experimental

The silicon materials used in this investigation were 2 in. diam n-type wafers with a resistivity of 3-7 Ω-cm. Wafers were about 300 μm thick and one side was mechanically and chemically polished.

Deposition processes were carried out at temperatures of 900°-1050°C while the liquid BBr_3 source was kept at 16°C which corresponds to a partial pressure of 42 Torr. High purity nitrogen was bubbled

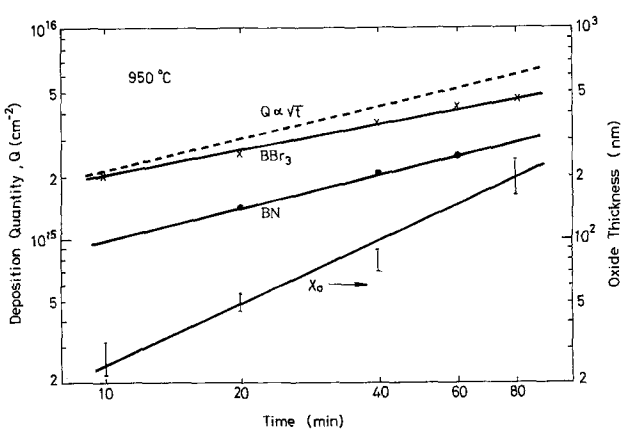

Fig. 1. Boron deposition quantity and oxide thickness as a function of time at 950°C.

* Electrochemical Society Active Member.
Key words: diffusion, boron deposition, BBr_3 source.

Downloaded on 2014-04-28 to IP 140.113.38.11 address. Redistribution subject to ECS terms of use (see ecsdl.org/site/terms_use) unless CC License in place (see abstract).

through the liquid and mixed with the main carrier gas consisting of nitrogen and oxygen.

The deposition cycle consisted of a 5 min preheating (N_2 and O_2), a given time of deposition (BBr_3 plus N_2 and O_2), and followed by a 1 min flush (N_2 and O_2). The gas flow rate was kept at N_2 1000 cm³/min, O_2 30 cm³/min, and $N_2 + BBr_3$ 10 cm³/min. The gas composition was estimated as O_2 3% and BBr_3 0.05%.

The deposition of boron in silicon was actually a very complicated oxidation-diffusion process. It consisted of a preliminary reaction of BBr_3 with O_2 which results in the chemical deposition of boric oxide on the silicon wafers

$$4BBr_3 + 3\,O_2 \rightleftharpoons 2B_2O_3 + 6Br_2 \qquad [1]$$

an interface reaction of oxygen with silicon to form silicon dioxide as well as some interstitial silicons (3)

$$Si + O_2 \rightarrow SiO_2 \qquad [2]$$

a reaction of boric oxide with silicon to produce silicon dioxide and boron atoms

$$2B_2O_3 + 3Si \rightleftharpoons 3SiO_2 + 4B \qquad [3]$$

and a possible etch of silicon by bromine

$$Si + 2Br_2 \rightarrow SiBr_4 \qquad [4]$$

Boric oxide was a liquid at normal deposition temperatures. It mixed readily with the silicon dioxide on the silicon surface to form a boro-silicate glass. Boron atoms deposited would diffuse into silicon or form a boron-rich surface layer.

After the deposition operation, the boro-silicate glass on the surface was etched with dilute HF, while the boron-rich layer as generally detectable by its hydrophilic behavior was removed boiling the wafer in the nitric acid (1). The thickness of some boro-silicate glasses was measured by a Rudolph Auto EL-II ellipsometer. The glass thickness as a function of time at 950°C is also shown in Fig. 1. The sheet resistance of the boron-deposited layer was measured using a Veeco Model FPP-100 four-point probe with a light weight. Each sample was measured on several points for many times to obtain an average value. The sheet resistance of the deposited layers as a function of time for various temperatures is shown in Fig. 2. Generally the junction depth of the deposited layers is very shallow. The junction depth was measured from a Solid State Measurements ASR-100B spreading resistance probe. To avoid a rounding effect, the silicon surface was coated with a layer of oxide by low temperature chemical vapor deposition. The junction depth of the deposited layers as a function of time for various temperatures is shown in Fig. 3.

The impurity profile was determined from the anodic sectioning technique. Anodic oxidation was carried out with a constant current source by using as electrolyte a solution of

$$HOCH_2CH_2OH : KNO_3 : H_2O / 1\ \text{liter} : 404\ \text{mg} : 20\ \text{ml}$$

The thickness of each oxide layer was measured by an ellipsometer. The sheet resistance after oxide stripping was measured by a four-point probe.

The measured data of the oxide thickness and the sheet resistance were converted to an impurity concentration profile through a computer program (7). The volumetric ratio for silicon converted to silicon dioxide was taken as 0.4 for anodic oxidation. The hole mobility-boron concentration relation established by Antoniadis *et al.* (8) was used in this work. To avoid the error magnification commonly found in discrete data differentiation, the measured data of the sheet resistance *vs.* distance were smoothed through fitting the logarithmic values of each five data points to a parabola by a standard least squares technique. The profiles of boron concentration in silicon at different temperatures for the same deposition time (20 min) and those at the same temperature (950°C) for various times are shown in Fig. 4 and 5, respectively.

Diffusion Model

The deposition of boron in silicon by using a BBr_3 source under an oxidizing ambient is an oxidation-diffusion process depicted in Fig. 6. Actually, this is a moving boundary problem and, in general, there is no analytic solution. Therefore, a numerical method should be used to generate a computer solution (9). Furthermore, a moving coordinate system is chosen to solve the moving boundary problem encountered in this work. As usual, the space and time are discretized into intervals of Δy and Δt. The impurity concentration C_j is evaluated at a node lying in the middle of each discrete cell j. The impurity flux $F_{j+1/2}$ is evaluated at the boundary between cells j and j + 1. As time changes from t_o to $t = t_o + \Delta t$, the oxide thickness increases from X_o^0 to X_o and the oxide-silicon interface as well as all cell boundaries will translate a distance $\Delta X = V\Delta t$, where V is the velocity of silicon consumed to form the oxide. An implicit scheme of the finite difference method is more suitable for solving this moving boundary problem. In a discretized form, the impurity flux may be written as (9)

$$F_{j+1/2} = (D_jC_j - D_{j+1}C_{j+1})/\Delta y \qquad [5]$$

where D_j and C_j are diffusivity and concentration of a

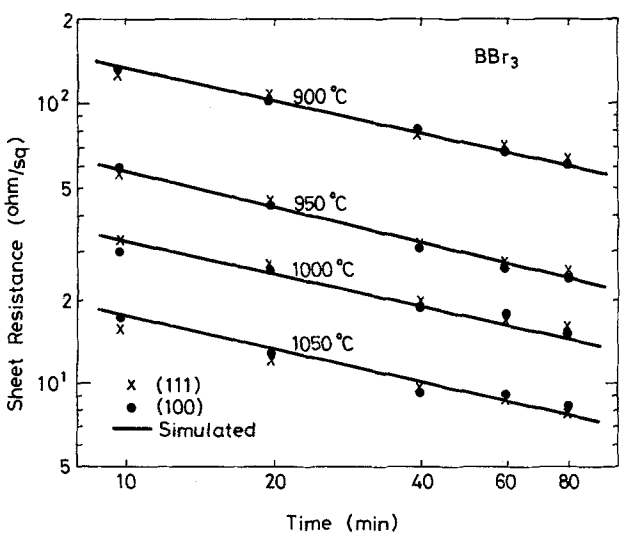

Fig. 2. Measured and simulated sheet resistances as a function of time for various temperatures.

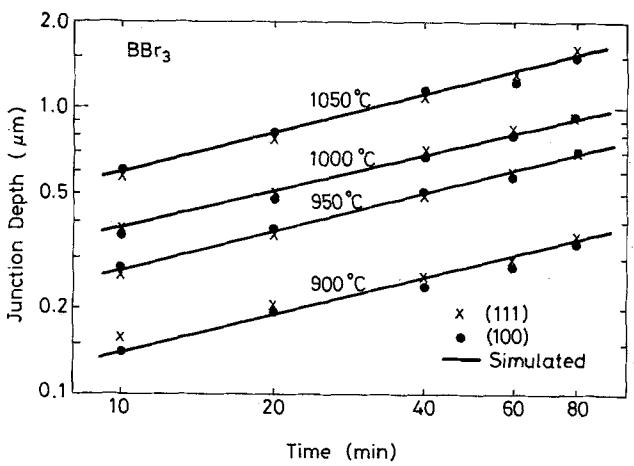

Fig. 3. Measured and simulated junction depths as a function of time for various temperatures.

Downloaded on 2014-04-28 to IP 140.113.38.11 address. Redistribution subject to ECS terms of use (see ecsdl.org/site/terms_use) unless CC License in place (see abstract).

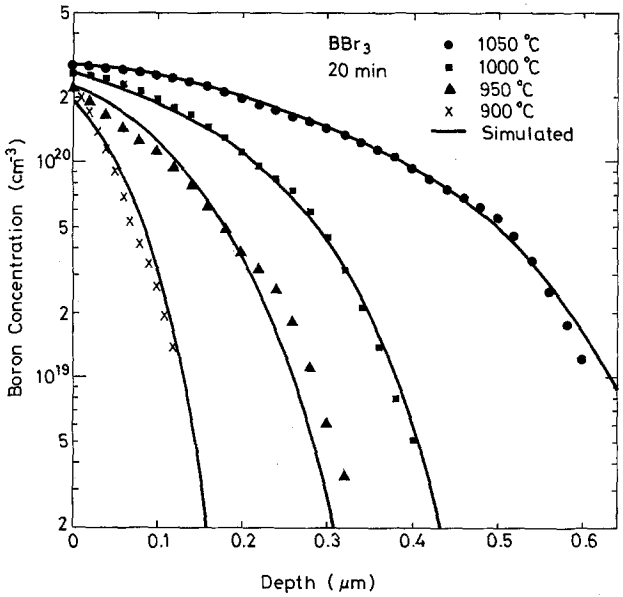

Fig. 4. Measured and simulated boron concentration profiles in silicon deposited for 20 min at various temperatures.

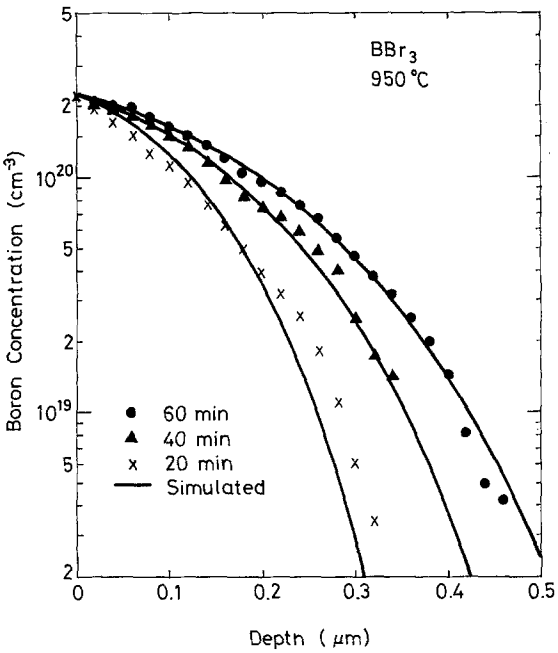

Fig. 5. Measured and simulated boron concentration profiles in silicon deposited at 950°C for various times.

j cell evaluated at time t. The continuity equation is given as

$$\frac{C_j - C_j'}{\Delta t} = \frac{F_{j-1/2} - F_{j+1/2}}{\Delta y} \qquad [6]$$

where C_j' is the average concentration of the j cell evaluated at time t_o with boundaries moved to the new positions at time t. From Fig. 6 it is easy to show that

$$C_j' = C_j^0 - (C_j^0 - C_{j+1}^0)\Delta x/\Delta y \qquad [7]$$

where C_j^0 is the concentration of the j cell at time t_o.

The cells at the two extreme boundaries deserve special attention. As shown in Fig. 6, the first discrete cell is actually a half-cell with its node at the oxide-silicon interface. The surface concentration C_S is assumed to be maintained at a constant value that corresponds to the solubility of boron in silicon in equilibrium with the concentration of boric oxide in the borosilicate glass.

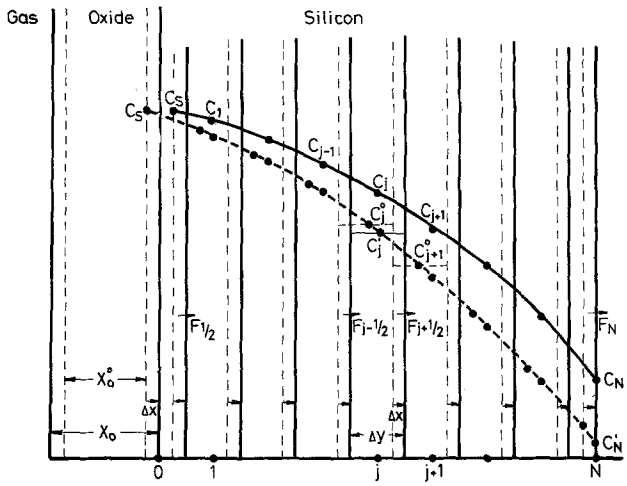

Fig. 6. A schematic diagram for boron deposition with a discretized moving coordinate.

The deep boundary usually lies inside the silicon substrate at the point where the simulated space terminates. The last cell in this end is also a half-cell similar to the first one. The impurity flux at the deep boundary F_N is taken as zero in the simulation program.

Results and Discussion

Measured values of the sheet resistance and junction depth of deposited layers as a function of time for various temperatures as well as measured profiles of boron in silicon at different temperatures and times can be simulated by properly choosing the boundary condition and modeling the diffusion coefficient. Simulated results are also illustrated in Fig. 2-5. The simulated values of surface concentration, moving boundary velocity, and diffusion coefficients as a function of temperature are given in Table I.

Surface concentration.—As shown in Fig. 4 and 5, simulated values of the surface concentration are in good agreement with the measured data. The results obtained in this work as well as those reported by Armigliato *et al.* (10) are shown in Fig. 7.

Moving boundary velocity.—The oxide-silicon interface is moved with a velocity V by the reactions of oxygen, boric oxide, and bromine to consume silicon as well as boron atoms. The reactions of oxygen and boric oxide with silicon, Eq. [2] and [3], result in the growth of silicon dioxide. The growth rate of silicon dioxide due to oxygen is generally given as (11)

$$v_1 = \frac{B_1}{2X_o + A_1} \qquad [8]$$

where B_1 and A_1 are the parameters defined by Deal and Grove (11). For thin oxide, $2X_o << A_1$, the oxidation rate is linearized as

$$v_1 \simeq B_1/A_1 \qquad [9]$$

The oxidation rate may be enhanced by a catalytic action (12) in the presence of bromine. It may also be enhanced by the high vacancy concentration generated in a heavily doped silicon (4, 13).

Table I. Some parameters used in profile simulations

T (°C)	900	950	1000	1050
C_S (cm^{-3})	1.9×10^{20}	2.3×10^{20}	2.6×10^{20}	2.9×10^{20}
V (cm/sec)	1.52×10^{-9}	2.24×10^{-9}	4.8×10^{-9}	8.0×10^{-9}
D_V^* (cm^2/sec)	1.21×10^{-15}	5.15×10^{-15}	1.96×10^{-14}	6.76×10^{-14}
γ	5.1	4	1.3	0.8

Downloaded on 2014-04-28 to IP 140.113.38.11 address. Redistribution subject to ECS terms of use (see ecsdl.org/site/terms_use) unless CC License in place (see abstract).

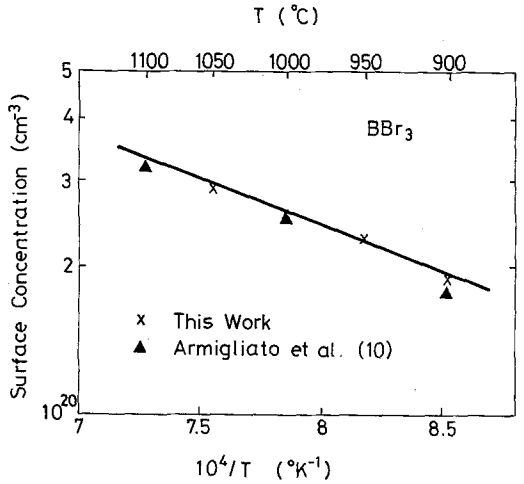

Fig. 7. Surface concentration of boron in silicon as a function of deposited temperature.

Due to oxidation enhancements as well as chemical deposition of boric oxide, Eq. [1], the oxide formation rate v_o estimated from the oxide thickness given in Fig. 1 is much larger than v_1 calculated from Eq. [9] using the parameters given by Deal and Grove (11). It is interesting to note that the ratio of silicon consuming rate V given in Table I to oxide formation rate v_o is around 0.55 which is slightly higher than the volumetric ratio of 0.45 for silicon converted to silicon dioxide during thermal oxidation. The difference may be attributed to the etching of silicon by bromine in the deposition process.

Diffusion coefficient.—From the study of oxidation-enhanced diffusion of boron and phosphorus in silicon, it is generally believed (14, 15) that a substitional impurity diffuses via a dual mechanism of vacancy and interstitialcy. An increase in the concentration of either vacancies C_V or interstitials C_I would cause the enhancement of impurity diffusion. Thus it is reasonable to assume that the effective diffusivity of an impurity may be expressed as

$$D = f_e(D_V + D_I) \qquad [10]$$

where f_e is the high concentration field enhancement factor given by (16)

$$f_e = 1 + [1 + (2n_i/C)^2]^{-1/2} \qquad [11]$$

D_V and D_I are the vacancy and interstitialcy motivated diffusivities given by (14)

$$D_V = D_V^* C_V/C_V^* \qquad [12]$$

$$D_I = D_I^* C_I/C_I^* \qquad [13]$$

with the asterisk denoting the corresponding intrinsic value.

The normalized vacancy concentration has been shown to follow the multiple charge state vacancy statistics (2, 4) and can be expressed as a function of hole concentration p as

$$\frac{C_V}{C_V^*} = \frac{1 + \beta^+(p/n_i) + \beta^-(n_i/p) + \beta^=(n_i/p)^2}{1 + \beta^+ + \beta^- + \beta^=} \qquad [14]$$

where β^+, β^-, and $\beta^=$ are the vacancy statistics parameters defined in Ref. (2).

The normalized concentration of self-interstitials has been related to the oxidation rate by a number of investigators (5, 6, 15) and can be expressed as

$$\frac{C_I}{C_I^*} = Kv_1^{\nu} \qquad [15]$$

where K is a proportional factor and ν is an exponent around 0.5 (3). Although v_1 is time dependent in general, Eq. [8], we will consider it as a constant, Eq. [9]. Substituting Eq. [12], [13], and [15] into Eq. [10], we obtain

$$D = f_e D_V^*(C_V/C_V^* + \gamma) \qquad [16]$$

where

$$\gamma = D_I^* K v_1^{\nu}/D_V^* \qquad [17]$$

is the interstitialcy contribution parameter with simulated values given in Table I. The intrinsic diffusivity reported by Fair (17) has been taken as D_V^* in this work. The intrinsic carrier concentration n_i which appears in Eq. [11] and [14] is calculated from Morin and Maita's empirical relation (18).

Doping composition effect.—The dependence of boron concentration profiles on doping gas composition can be modeled by the change of interstitialcy contribution parameter γ. Higher oxygen flow rate results in higher oxidation rate v_1 and hence higher interstitial concentration C_I. While higher BBr_3 concentration produces higher boric oxide concentration in the oxide layer which reacts with the excess silicon at the interface. Therefore the interstitial concentratiion C_I is reduced and a boron-rich layer (BRL) is formed at silicon surface.

Figure 8 reproduces the measured profiles of Negrini *et al.* (1) at 1000°C for 23 min with different gas compositions. The observed differences in the surface concentration can be modeled by the displacement δ of the BRL-Si interface from the original oxide-silicon interface. The simulated results for boron concentration profiles with different values of γ and δ are also shown in the figure. A constant surface concentration of 2.6×10^{20} cm^{-3} is taken at the oxide-silicon interface and the origins of all profiles are taken at the BRL-Si interface. Good agreement in profile shapes as well as deposition quantities has been obtained.

Deposition quantity.—The quantity Q of boron deposited in silicon can be determined in some cases by numerical integration of the measured doping profiles. However, as revealed from profile and sheet resistance simulations, the average mobilities of deposited layers are very close together (54.3 ± 1.1 cm^2/V-sec) and a sufficiently accurate value of Q can be obtained from the measured sheet resistance. Figure 1 shows the deposition quantity Q as a function of time at 950°C for BBr_3 and BN sources. Also shown in the figure is a

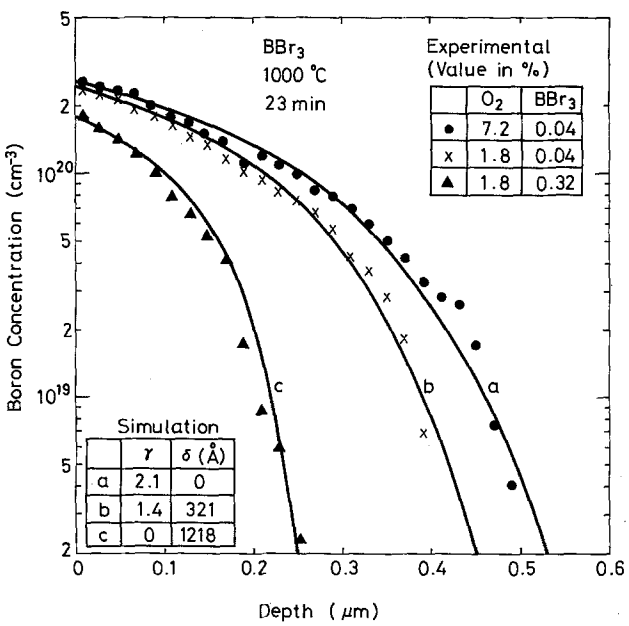

Fig. 8. Measured and simulated boron concentration profiles in silicon deposited at 1000°C for 23 min with different doping gas compositions.

Downloaded on 2014-04-28 to IP 140.113.38.11 address. Redistribution subject to ECS terms of use (see ecsdl.org/site/terms_use) unless CC License in place (see abstract).

relation of $Q \propto t^{1/2}$ which is obtained by taking the moving boundary velocity V as zero.

Conclusion

The sheet resistance and junction depth of boron-deposited layers as a function of time for various temperatures using a BBr_3 source can be simulated by properly choosing the boundary conditions and modeling the diffusion coefficient. The diminishing of the deposition quantity is modeled by a moving velocity of the oxide-silicon interface. The increase of the deposition quantity by using BBr_3 as compared to BN is attributed to the formation of silicon self-interstitials. The gas composition dependence of boron deposition is explained by the change of the interstitialcy contribution as well as the formation of a boron-rich layer.

Acknowledgments

The helpful discussions with Dr. W. P. Wang are highly appreciated. The authors are also grateful for the assistance by the staff of Semiconductor Research Laboratory of Tatung Institute of Technology in the impurity concentration profile measurements. This research work was sponsored through National Science Council Contract No. NSC70-0404-E009-03.

Manuscript submitted Aug. 31, 1981; revised manuscript received Dec. 18, 1981.

Any discussion of this paper will appear in a Discussion Section to be published in the June 1983 JOURNAL. All discussions for the June 1983 Discussion Section should be submitted by Feb. 1, 1983.

Publicatiion costs of this article were assisted by the National Chiao Tung University.

REFERENCES

1. P. Negrini, A. Ravaglia, and S. Solmi, *This Journal*, **125**, 609 (1978) and references therein.
2. S. F. Guo, *ibid.*, **127**, 2506 (1980).
3. R. B. Fair, *ibid.*, **128**, 1360 (1981) and references therein.
4. C. P. Ho and J. D. Plummer, *ibid.*, **126**, 1516 (1979).
5. S. M. Hu, *J. Appl. Phys.*, **45**, 1567 (1974).
6. A. M. Lin, D. A. Antoniadis, and R. W. Dutton, *This Journal*, **128**, 1131 (1981).
7. J. C. Plunkett, J. L. Stone, and A. Leu, *Solid State Electron.*, **20**, 447 (1977).
8. D. A. Antoniadis, A. G. Gonzaley, and K. W. Dutton, *This Journal*, **125**, 813 (1978).
9. D. A. Antoniadis, M. Rodoni, and R. W. Dutton, *ibid.*, **126**, 1939 (1979).
10. A. Armigliato, D. Nobili, P. Ostoja, M. Servidori, and S. Solmi, in "Semiconductor Silicon 1977," H. R. Huff and E. Sirtl, Editors, p. 638, The Electrochemical Society Softbound Proceedings Series, Princeton, NJ (1977).
11. B. E. Deal and A. S. Grove, *J. Appl. Phys.*, **36**, 3770 (1965).
12. K. Hirabayashi and J. Iwamura, *This Journal*, **120**, 1595 (1973).
13. J. D. Plummer, in "Semiconductor Silicon 1981," H. R. Huff, R. J. Kriegler, and Y. Takeishi, Editors, p. 445, The Electrochemical Society Softbound Proceedings Series, Pennington, NJ (1981).
14. D. A. Antoniadis, in "Semiconductor Silicon 1981," H. R. Huff, R. J. Kriegler, and Y. Takeishi, Editors, p. 947, The Electrochemical Society Softbound Proceedings Series, Pennington, NJ (1981).
15. K. Taniguchi, K. Kurosawa, and M. Kashiwagi, *This Journal*, **127**, 2243 (1980).
16. K. Lehovec and A. Slobodskoy, *Solid State Electron.*, **3**, 45 (1961).
17. R. B. Fair, *This Journal*, **122**, 800 (1975).
18. F. J. Morin and J. P. Maita, *Phys. Rev.*, **96**, 28 (1954).

Studies of Methacrylonitrile and Trichloroethyl Methacrylate Copolymers as Electron Sensitive Positive Resists

J. H. Lai

Honeywell Corporate Technology Center, Bloomington, Minnesota 55420

and J. H. Kwiatkowski and C. F. Cook, Jr.

U.S. Army Electronics Technology and Devices Laboratory, Fort Monmouth, New Jersey 07703

ABSTRACT

Positive electron resists derived from copolymers of methacrylonitrile (MCN) and trichloroethyl methacrylate (TCEM) have been synthesized, characterized, and evaluated. The sensitivity of 2:1 MCN/TCEM copolymer is 5 μC cm^{-2} with 40% unexposed area thickness loss. The plasma etch resistance of the copolymer is significantly higher than that of the TCEM homopolymer. The inclusion of the comonomer MCN, however, has not significantly broadened the exposure range for the copolymer as a positive-acting resist. The copolymer resists exhibited significant concurrent cross-linking at a dose $\geq$ 20 μC cm^{-2}.

Poly(methacrylonitrile) (PMCN) is one of the vinyl polymers that is highly sensitive to high energy radiation. On exposure to high energy electron beams, chain scission occurs predominantly in the polymer with negligible concurrent cross-linking. The G_s value, defined as the number of chain scission events per 100 eV of energy absorbed, of PMCN has been reported to be 3.3 (1). The value is significantly higher than 1.6 of PMMA [poly(methyl methacrylate)], the current standard E-beam resist. The thermal stability of the polymer is also better than PMMA. The glass transition temperature (T_g) of PMCN is 120°C (2), which is higher than the T_g of PMMA, which is 100°C. Further, it has been shown that PMCN is one of the few aliphatic vinyl polymers that has high plasma etch resistance (3).

Although PMCN has the attractive properties discussed above, the polymer has one major drawback. The polymer is highly solvent resistant (4). The poor solubility of the polymer has resulted in the use of less common solvents, *e.g.*, nitromethane and benzonitrile, for spin coating and development of the polymer resist (5). The poor solubility of the polymer also hinders the possibility of further enhancing the resist sensitivity through optimization of the development process.

Key words: positive electron resist, methacrylonitrile, trichloroethyl methacrylate, copolymer.

Downloaded on 2014-04-28 to IP 140.113.38.11 address. Redistribution subject to ECS terms of use (see ecsdl.org/site/terms_use) unless CC License in place (see abstract).